Eshelby Twist and Magic Helical Zinc Oxide Nanowires and Nanotubes

E. Akatyeva and T. Dumitrică

Department of Mechanical Engineering, University of Minnesota, Minneapolis, Minnesota 55455, USA

(Received 25 December 2011; published 16 July 2012)

Twisted zinc oxide nanowires and nanotubes were recently synthesized by screw-dislocation growth. We show theoretically that once their diameter increases above a critical size of the order of a few atomic spacings, the existence of these structures can be rationalized in terms of the energetics of surfaces and veritable Eshelby's twist linear elasticity mechanics supplemented by a nonlinear core term. For Burgers vector larger than the minimum allowed one, a twisted nanotube with well-defined thickness, rather than a nanowire, is the most stable nanostructure. Results are assistive for designing ultrathin nanostructures made out of nonlayered materials.

DOI: 10.1103/PhysRevLett.109.035501 PACS numbers: 61.46.Np, 61.72.Lk

Recent experimental advances have provided an unprecedented level of control in the synthesis of nanowire (NW) and nanotube (NT) of zinc oxide (ZnO) [1,2] and other materials [3–5] grown by engaging dislocations, where a seeded axial screw dislocation of a well-defined Burgers vector provides the self-perpetuating steps for enabling the quasi-one-dimensional growth. ZnO NTs, which possess a regular wurtzite structure, appear to grow into twisted structures of well-defined sizes, such as NTs with $R = 12.6$ nm and $r = 2.9$ nm outer and inner radii, respectively [1]. This class of anisotropic structures are exciting for many reasons. Twisted NWs and NTs with finite thickness made out of nonlayered materials represent a novel organization of matter, similar but not identical to multiwalled NTs made out of layered materials. The way in which a screw dislocation influences the stability and properties of these nanostructures remains an open and important problem.

The open-core elastic dislocation model of Frank [6] and the elastic Eshelby model predicting the macroscopic twist undergone by a thin rod [7,8] containing a screw dislocation provide a starting point for understanding the structural transition from screw-dislocated NWs to NTs. For large Burgers vectors, it is energetically more favorable for dislocation to become hollow by removing the crystalline material adjacent to the dislocation line and creating an additional surface in the form of a hollow tube. Nonetheless, the detailed stabilization mechanism leading to the observed NTs is unknown mainly because the applicability of the Eshelby model to screw-dislocated nanostructures is not warranted by recent experimentation [4,9]. In twisted PbSe NWs with R in the 30–50 nm range [4], the estimation of the Burgers vector magnitude using the Eshelby model [7] indicated a large value [9], attributed by those authors to the presence of a super screw dislocation. In InP NWs with $R = 10$ nm, the measured twist rate exceeded by up to 100% the value estimated with the Eshelby model [7] based on the minimal Burgers vector [9]. This result was interpreted as a significant deviation from the macroscopic behavior.

ZnO is the material of choice for the present investigation because the stability and properties of pristine ZnO NWs and NTs have been well explored [10–14], particularly through microscopic simulation. Unfortunately, screw-dislocated nanostructures are not within the reach of standard microscopic approaches. Therefore, investigating the connection between thermodynamical stability and Eshelby's mechanics in these structures calls for a fresh approach. Indeed, twisted structures with a uniform helical symmetry have a unit cell size corresponding to the size of the helical motif. Such large number of atoms prohibits calculations adopting translational symmetry via periodic boundary conditions (PBC). Instead, here we employ objective molecular dynamics (MD) [15] coupled [16–18] with a density-functional based tight binding (DFTB) [19,20]. The valence shell basis set used here comprises sp basis functions for O and spd for Zn. In objective MD, we describe the infinitely long screw-dislocated NWs and NTs as objective structures [21] from basic repetition rules involving translations and rotations

$$\mathbf{X}_{j,\zeta} = \mathbf{R}^{\zeta}\mathbf{X}_j + \zeta\mathbf{T}. \quad (1)$$

Index j runs over the N_0 atoms at the positions $\mathbf{X}_j$ inside the objective domain (a screw-dislocated PBC domain), while index ζ labels various replicas of the domain. The helical operation applied to the objective domain is defined by the rotational matrix $\mathbf{R}$ of angle θ and the axial vector $\mathbf{T}$. As N_0 is small, adoption of the objective structures concept enables calculations that would otherwise be beyond reach. Moreover, with the symmetry-adapted treatment of the electronic states [16], the structural parameters $\mathbf{T}$ and θ can take arbitrary values, permitting us to find the optimal configuration via conjugate gradient relaxations. Two example calculations are shown in Figs. 1(a) and 1(b). The two screw-dislocated NTs of same stoichiometry, R, and Burgers vector magnitude,

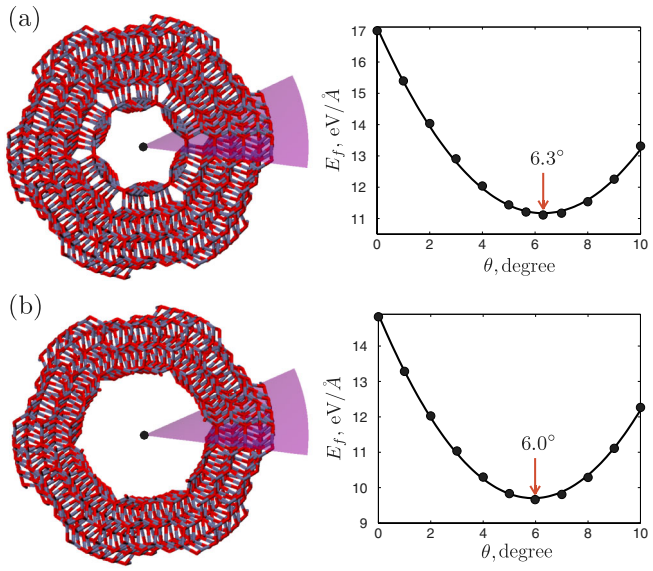

FIG. 1 (color online). Atomistic representations of the relaxed configurations (left) and plots of the formation energy versus the twist angle (right) for (a) $\{5, 1\}_{3b}$ and (b) $\{5, 2\}_{3b}$ ZnO NTs. The Eshelby twist angles of 6.3° and 6.0°, respectively, are indicated by down arrows. The outer radius is $R = 14.7$ Å. The purple (gray) plane is the cut made to create the dislocation. Note the intrinsic twist.

but different wall thickness, exhibit different intrinsic twist values and formation energies (E_f). The goal of this Letter is to establish a basis for systematically predicting the energetic stability of twisted NT and NW over a large range of diameters.

The ZnO wurtzite crystal presents a hexagonal lattice with parameters $a = 3.23$ Å and $c = 5.32$ Å along the basal plane and the vertical axis, respectively. Here we studied ZnO NTs and NWs with translational periodicity $\sim c$ (precise value was found by conjugate gradient energy minimizations) along the [0001] direction and bounded by six $\{10\bar{1}0\}$ surfaces. We focused on ultrathin structures since in this size limit any potential deviations from Eshelby model are maximal. In NWs, the number of layers L in the cross-section was varied from 2 to 6. There are two ways to define R, as Ld_{100} where $d_{100} = \sqrt{3}a/2$ is the distance between $(10\bar{1}0)$ planes, or as $(4L - 1)d_{110}/2$, where $d_{110} = a/2$ is the distance between $(11\bar{2}0)$ planes, where a is evaluated from the relaxed pristine configurations. We took R as the averaged values obtained with these two approaches. Then R ranged from 5.5 Å to 17.7 Å. From each pristine NW we created a collection of NTs by systematically removing inner atomic layers. These NTs can be uniquely denoted by $\{L, h\}$, where $h = 1, \ldots, L - 2$ is the number of missed inner atomic layers. (The particular $h = L - 1$ monolayer case deserves special attention and therefore it was considered in a separate work [17].) Here r was defined in an analogous manner with R and ranged from 2.6 Å to 11.8 Å.

The energetics of the optimized pristine NWs and NTs was analyzed using a standard Wulff decomposition of the E_f (measured per length) approach. E_f is defined as difference between the total and bulk energies. The functional form [15] of E_f contains surface, edge energy terms, and bulk strain energy correction, that captures the elastic strain stored in the NW or NT walls. By fitting it to our DFTB data, we determined that the last two components can be neglected, in agreement with what was previously found in hexagonal Si NW [16]. Thus, E_f contains only the surface energy term $2\pi\gamma(R + r)$, with a surface energy value $\gamma = 64.3$ meV/Å^2. It is worth noting that γ compares well with the DFTB value of 63.2 meV/Å^2 and the *ab initio* value of 72.4 meV/Å^2 [22] for the $(10\bar{1}0)$ surface of bulk ZnO.

As in the experiment detailed in Ref. [9], we explored screw dislocations with Burgers vectors **b** of the minimum allowable length c, and triple that magnitude as a model for a super-screw dislocation. The presence of an axial screw dislocation is denoted by a subscript giving the magnitude of the Burgers vector as $\{L, h\}_{kb}$, where $k = 1$ and 3. To rationalize the NW core-surface interaction, we considered the location of the dislocation core at the NW center as well as at a distance ξ away. One immediately recognizes that E_f contains two terms: a surface energy and a strain energy of the dislocation E_d term. Since the dislocations do not change the surface energy, E_d is obtained by subtracting E_f of the pristine structure from the dislocated one. The E_d term will be addressed next.

We first discuss dislocated ultrathin NWs. It is reasonable to expect that due to the close vicinity of surfaces, NWs would eject the dislocation to revert to the pristine structure. However, there is convincing evidence that they remain stable [3,4,9]. We directly probed the stability of the screw-dislocated NWs and the role of twisting by carrying out two separate constant energy MD simulations under both PBC and stress-free objective boundary conditions. A number of 108 atoms located in the primitive cell of a $\{3, 0\}_b$ were evolved in time for 5.5 ps with a time step of 1 fs. Although the initial temperature (T) was in both cases 400 K, the two simulations led to different outcomes. On the one hand, in the PBC MD solution, the screw dislocation is gradually ejected from the untwisted NW, Fig. 2(a), until the lowest-energy pristine structure is regained. The dynamics of this process can be followed in animation 1 of the Supplemental Material [23] and is reflected in the dramatic increase in instantaneous T in Fig. 2(b), that signifies a lowering of the potential energy. On the other hand, the objective MD solution retains the dislocation axis at the center of the NW twisted by 1.26 deg/Å. This dynamical process can be visualized in animation 2 [23] and is reflected in the equilibrium T fluctuations of Fig. 2(c).

The contrasting dynamical behavior observed above is further supported by the strain energy data for a collection

of $\{L, 0\}_b$ NWs when the dislocation core is located at various ξ. In Fig. 2(d) it can be seen that when the twist is neglected (as under PBC), the axis ($\xi = 0$) location is unstable. When the intrinsic twist effect is considered by the objective boundary conditions, the $\xi = 0$ location becomes stable. Only when the core is displaced halfway from the surface can the dislocation be ejected. The intrinsic twist dependence on ξ is shown in Fig. 2(e).

We note that objective MD ability to accurately account for the small intrinsic twist enables the understanding the stability of these NWs. From a different perspective, our microscopic findings are in excellent agreement with the elastic theory predictions: a dislocation is stable at the center of a cylinder with stress-free surfaces only when it is allowed to undergo an Eshelby twist. Here E_d (per unit length) produced by an axial screw dislocation in a cylindrical rod ($r = 0$) of radius R writes as [7]

$$E_d = E_c + \frac{Gb^2}{4\pi}\left[\ln\frac{R}{r_c} + \ln\left(1 - \frac{\xi^2}{R^2}\right) - \left(1 - \frac{\xi^2}{R^2}\right)^2\right]. \quad (2)$$

Here E_c and r_c represent the nonclassical core energy (per unit length) and the core size of the dislocation while G is the shear modulus. The first two terms in brackets are caused by the screw dislocation elastic strain field while the last term captures the energy gained by acquiring the twist rate

$$\alpha_\xi = \frac{b}{\pi R^2}\left(1 - \frac{\xi^2}{R^2}\right). \quad (3)$$

Of course, this continuum treatment cannot be applied within the dislocation core region characterized by high lattice distortions. Nevertheless, both r_c and E_c can be determined from the objective MD data [17]. We determined r_c by comparing the relaxed configuration and the structure generated by displacing atoms according to continuum strain field of a dislocation. Defining the dislocation core by the region with the highest (greater than 0.4 Å) relative displacements between these two configurations, we obtained $r_c = 2a/\sqrt{3} = 3.73$ Å, as also depicted by the hatched areas in Fig. 2(a). By fitting Eq. (2) to our data with $\zeta = 0$ we obtained $E_c = 1.29$ eV/Å and $G = 51$ GPa, which is in good agreement with the bulk value of 44 GPa [24]. For a comprehensive comparison, we plot in Figs. 2(d) and 2(e) shifted strain energy E_ξ, where the R dependence is eliminated by subtracting $(Gb^2/4\pi)\ln(R/r_c)$ term from Eq. (2), and rescaled twist rate versus the dislocation line position. The surprisingly good agreement between our atomistic data and continuum predictions brings the fortunate conclusion that Eshelby's theory remains valid even with regard to ultrathin screw-dislocated ZnO NWs.

The way the dislocation affects the electronic states should be interesting to pursue. In objective calculations, the electronic states are indexed by the helical quantum number κ, Fig. 3(a), instead of the linear momentum k used under PBC, Fig. 3(b). Most notably, we find that the core of the screw dislocated NWs couples directly to the electronic states around the Fermi level. For the case of $R = 8.6$ Å NW of Fig. 3, the first empty LUMO band located on the core of the dislocation reduces significantly the direct band gap from 3.3 eV (pristine NW) to 2.6 eV.

We now discuss dislocated NTs. Using continuum [8], we can quantify with confidence E_d and the stabilizing twist rate. When $r > r_c$, i.e., when $h \geq 2$,

$$E_f = 2\pi\gamma R\left(1 + \frac{r}{R}\right) + \frac{Gk^2b^2}{4\pi}\left[\ln\frac{R}{r} - \frac{1 - r^2/R^2}{1 + r^2/R^2}\right], \quad (4)$$

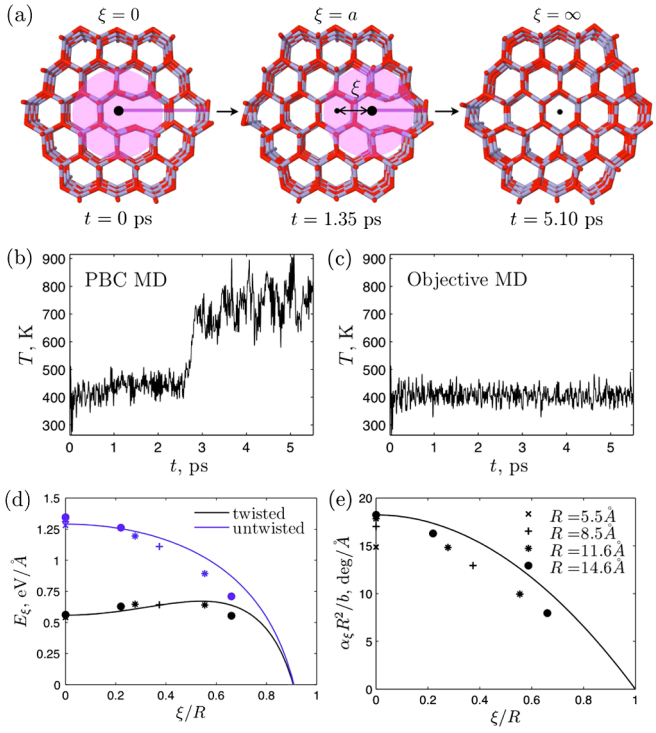

FIG. 2 (color online). (a) Snapshots from PBC MD simulations of a $\{3, 0\}_b$ ZnO NW. The hatched area depicts the dislocation core region. Instantaneous temperature from MD simulations (b) under PBC and (c) objective boundary conditions. The graphs of the shifted strain energy E_ξ for twisted and untwisted ZnO NWs (d) and rescaled twist rate (e) versus the dislocation line position. Microscopic data and continuum predictions are shown with symbols and lines, respectively.

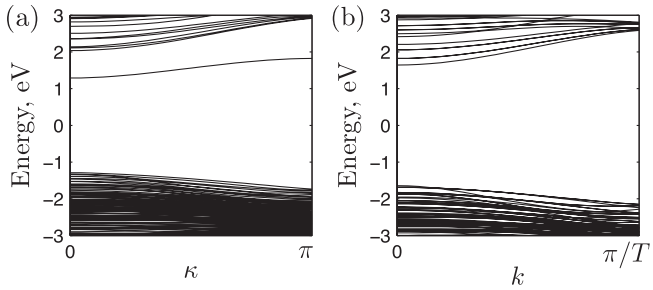

FIG. 3. Comparison for the electronic band structure of (a) $\{3, 0\}_b$ and (b) $\{3, 0\}$ ZnO NWs.

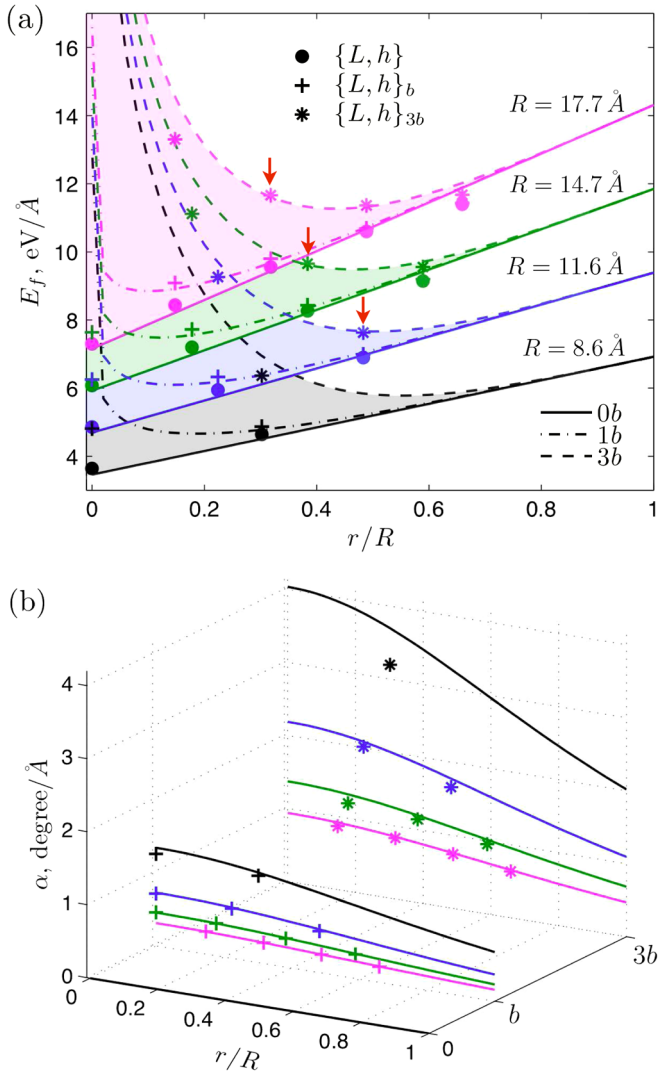

FIG. 4 (color online). (a) Formation energy and (b) intrinsic twist rate for ZnO NTs with different Burgers vector magnitudes, $0b$ (pristine structures), $1b$, and $3b$, versus the ration r/R. NTs with equal outer radii R are shown in the same color. Lines correspond to Eqs. (4) and (5) and symbols are the microscopic data. Arrows indicate the "magic" twisted NT structures.

and

$$\alpha = \frac{kb}{\pi R^2}\frac{1}{1 + r^2/R^2}. \quad (5)$$

Interestingly, Eqs. (4) and (5) were shown to hold even in the one-atom thick NT limit [18]. Figures 4(a) and 4(b), showing the formation energy and twist rate for ZnO NTs as a function of r/R for different R, demonstrate good agreement between the current simulation data (symbols) and the curves given by the continuum model. Recall that in pristine NTs, E_f contains only the surface term, in dislocated NTs E_f contains also E_d captured by the second term in Eq. (4). Hence, at constant R, the differences between the dislocated and pristine curves in Fig. 4(a) are attributed to E_d. For the super screw dislocation, the interplay between the surface and dislocation strain energies delineates a local minimum. The closest discrete realization corresponds to a favorable NT with a well-defined wall thickness [see down arrows in Fig. 4(a)]. This kind of argument should be relevant to the observed NTs [1,2] since the continuum theory is readily applicable at larger sizes. However, for the NTs with minimal Burgers vector we find no thermodynamic minima with $r > r_c$. As in pristine NTs, E_f is dominated by the inner surface energy term. Since $E_c < 2\pi r_c \gamma$, $\{L, 0\}_b$ NWs appear more favorable than $\{L, h\}_b$ NTs. When $r < r_c$, our predictive framework no longer holds as the continuum leads to divergences, Fig. 4(a). To gain insight into this small region, we make recourse solely to our DFTB direct calculations which obtained that $\{L, 0\}_b$ NWs are slightly more stable than corresponding $\{L, 1\}_b$ NTs.

In conclusion, using the method of objective MD, we have simulated ultrathin ZnO NWs and NTs with a wurtzite structure containing a screw dislocation and showed that the competition between the lattice strain and surface energy leads to ultrathin chiral NTs made out of nonlayered materials. While accessible in experiment, the characterization of the Burgers vector and atomic structure distortions associated with lattice twisting presents many challenges and sources of errors. At variance with recent experimentation [9], we conclude here that the continuum Eshelby model works very well above a critical size of only a few atomic spacings. This validation opens up the possibility for understanding the stability of a class of nanomaterials [1–5] with new properties and diverse applications. Our result is in good agreement in all important respects with the recent ZnO NT experiments [1,2]. For example, Eq. (4) predicts that the observed twisted ZnO NTs with $r = 2.9$ nm and $R = 12.6$ nm should store a large Burgers vector of 2.4 nm magnitude, a value that compares well with the reported [1] 1.94 nm.

We thank G. Seifert for providing us the DFTB parameters. We acknowledge support from NSF CAREER Grant No. CMMI-0747684 and the University of Minnesota. Computations were carried out at the Minnesota Supercomputing Institute.

[1] S. A. Morin, M. J. Bierman, J. Tong, and S. Jin, Science **328**, 476 (2010).
[2] S. A. Morin and S. Jin, Nano Lett. **10**, 3459 (2010).
[3] M. J. Bierman, Y. K. Albert Lau, A. V. Kvit, A. L. Schmitt, and S. Jin, Science **320**, 1060 (2008).
[4] J. Zhu, H. Peng, A. F. Marshall, D. M. Barnett, W. D. Nix, and Y. Cui, Nature Nanotech. **3**, 477 (2008).
[5] F. Meng, S. A. Morin, and S. Jin, J. Am. Chem. Soc. **133**, 8408 (2011).
[6] F. C. Frank, Acta Crystallogr. **4**, 497 (1951).
[7] J. D. Eshelby, J. Appl. Phys. **24**, 176 (1953).
[8] J. D. Eshelby, Philos. Mag. **3**, 440 (1958);K. Youshida, Jpn. J. Appl. Phys. **3**, 565 (1964).

[9] L. H. G. Tizei, A. J. Craven, L. F. Zagonel, M. Tencé, O. Stéphan, T. Chiaramonte, M. A. Cotta, and D. Ugarte, Phys. Rev. Lett. **107**, 195503 (2011).
[10] J. H. Song, X. D. Wang, E. Riedo, and Z. L. Wang, Nano Lett. **5**, 1954 (2005).
[11] H. Xu, R. Q. Zhang, X. Zhang, A. L. Rosa, and Th. Frauenheim, Nanotechnology **18**, 485713 (2007).
[12] W. Fan, H. Xu, A. L. Rosa, Th. Frauenheim, and R. Q. Zhang, Phys. Rev. B **76**, 073302 (2007).
[13] G. Stan, C. V. Ciobanu, P. M. Parthangal, and R. F. Cook, Nano Lett. **7**, 3691 (2007).
[14] H. Pan and Y. P. Feng, ACS Nano **2**, 2410 (2008).
[15] T. Dumitrică and R. D. James, J. Mech. Phys. Solids **55**, 2206 (2007).
[16] D.-B. Zhang, M. Hua, and T. Dumitrică, J. Chem. Phys. **128**, 084104 (2008).
[17] I. Nikiforov, D.-B. Zhang, and T. Dumitrică, J. Phys. Chem. Lett. **2**, 2544 (2011).
[18] D.-B. Zhang, E. Akatyeva, and T. Dumitrică, Phys. Rev. B **84**, 115431 (2011); D.-B. Zhang, T. Dumitrica, and G. Seifert, Phys. Rev. Lett. **104**, 065502 (2010).
[19] N. H. Moreira, G. Dolgonos, B. Aradi, A. L. Rosa, and T. Frauenheim, J. Chem. Theory Comput. **5**, 605 (2009).
[20] R. Rurali and E. Hernandez, Comput. Mater. Sci. **28**, 85 (2003).
[21] R. D. James, J. Mech. Phys. Solids **54**, 2354 (2006).
[22] A. Wander and N. M. Harrison, Surf. Sci. Lett. **468**, L851 (2000).
[23] See Supplemental Material at http://link.aps.org/supplemental/10.1103/PhysRevLett.109.035501 for PBC MD and objective MD animations.
[24] T. B. Bateman, J. Appl. Phys. **33**, 3309 (1962).